

Threefold Cation– π Bonding in Trimethylsilylated Allyl Complexes

Cameron K. Gren,[†] Timothy P. Hanusa,^{*,†} and Arnold L. Rheingold[‡]

Department of Chemistry, Vanderbilt University, Nashville, Tennessee 37235, and Department of Chemistry and Biochemistry, University of California at San Diego, La Jolla, California 92093-0358

Received December 24, 2006

Reaction of zinc triflate with the lithium, sodium, and potassium salts of the bis(1,3-trimethylsilyl)-allyl anion, $M[A']$ ($A' = [1,3-(SiMe_3)_2C_3H_3]$), produces the triallylzincates $Li[ZnA'_3]$ (**1**), $Na[ZnA'_3]$ (**2**), and $K[ZnA'_3]$ (**3**) rather than the initially expected neutral ZnA'_2 . The molecules are fluxional in solution, and the chemical shifts of the molecules in C_6D_6 are different for the three molecules, indicating that the cations remain associated with the triallylzinc anion. Single-crystal X-ray structures of **2** and **3** reveal that the three allyl ligands are bound to the zinc in an arrangement with approximate C_3 symmetry, with the alkali-metal cations situated between the double bonds of the allyl ligands. The distances are consistent with noncovalent cation– π interactions. The structure of the lithium derivative **1** is similar to those of **2** and **3**, but the asymmetry in the metal–carbon distances suggests that some $Li-C$ σ -bonding is involved. Density functional theory calculations were performed on $[M(C_6H_6)]^+$ and $[M(C_2H_4)_n]^+$ ($M = Li, Na, K$; $n = 1-3$) cations with the PBE1PBE functional and basis sets of triple- ζ quality. The binding enthalpies (ΔH°) of the three metals to two ethylene molecules or to benzene are approximately the same, despite the latter's greater number of π -electrons. The binding energy of three ethylene molecules to the metal cations exceeds that of benzene by 30–50%, underscoring the importance of geometric factors to cation– π interactions.

Introduction

Cation– π interactions involve the largely noncovalent attraction of a cation (usually an alkali metal or NR_4^+ ; $R = H, Me$) with a ligand's π -electrons, which are commonly (although not necessarily) those in an aromatic ring (Figure 1a).¹ Several factors are thought to contribute to cation– π interactions, including electrostatic and dispersion forces and charge transfer/inductive effects.² The interaction energy can be substantial: that of K^+ with benzene in the gas phase (ca. 17.7 ± 1.0 kcal mol^{-1}),³ for example, is about the same as that with water (17.9 kcal mol^{-1}).⁴ Cation– π interactions with aromatic rings appear in numerous supramolecular and biological contexts, including cyclophanes,⁵ calixarenes,⁶ collarenes,⁷ polyaromatics,⁸ and

amino acids such as tryptophan.⁹ Even when weak, multiple cation– π (arene) interactions can critically influence ligand conformations and substrate binding.¹⁰

Instead of aromatic rings, the source of the electrons in cation– π interactions can be individual double and triple bonds,^{11–15} but less is known about structural and energetic features in such cases.¹⁶ The gas-phase $Na^+ \cdots C_2H_4$ interaction has been experimentally measured,¹¹ for example, and the cyclic beltene (cyclacenes) (Figure 1b) display size-selective binding of alkali-metal cations mediated by cation– π interactions.¹² π -Complexes of the d^{10} Ag^+ ion are sometimes classified as examples of cation– π interactions,¹³ but structural and theoretical characterization of species such as the $[Ag(C_2H_4)_3]^+$ ion¹⁷ and $Ag^+[2.2.2]$ cyclophane prisms¹⁸ indicates that d-orbital

* To whom correspondence should be addressed. E-mail: t.hanusa@vanderbilt.edu.

[†] Vanderbilt University.

[‡] University of California at San Diego.

(1) (a) Ma, J. C.; Dougherty, D. A. *Chem. Rev.* **1997**, *97*, 1303–1324. (b) Meyer, E. A.; Castellano, R. K.; Diederich, F. *Angew. Chem., Int. Ed.* **2003**, *42*, 1210–1250.

(2) Kim, D.; Hu, S.; Tarakeshwar, P.; Kim, K. S.; Lisy, J. M. *J. Phys. Chem. A* **2003**, *107*, 1228–1238.

(3) Amicangelo, J. C.; Armentrout, P. B. *J. Phys. Chem. A* **2000**, *104*, 11420–11432.

(4) Sunner, J.; Nishizawa, K.; Kebarle, P. *J. Phys. Chem.* **1981**, *85*, 1814–1820.

(5) (a) Bartoli, S.; Roelens, S. *J. Am. Chem. Soc.* **2002**, *124*, 8307–8315. (b) Sarri, P.; Venturi, F.; Cuda, F.; Roelens, S. *J. Org. Chem.* **2004**, *69*, 3654–3661.

(6) (a) Araki, K.; Shimizu, H.; Shinkai, S. *Chem. Lett.* **1993**, *2*, 205–208. (b) Arduini, A.; Pochini, A.; Secchi, A. *Eur. J. Org. Chem.* **2000**, 2325–2334. (c) Matthews, S. E.; Schmitt, P.; Felix, V.; Drew, M. G. B.; Beer, P. D. *J. Am. Chem. Soc.* **2002**, *124*, 1341–1353. (d) Matthews, S. E.; Rees, N. H.; Felix, V.; Drew, M. G. B.; Beer, P. D. *Inorg. Chem.* **2003**, *42*, 729–734.

(7) Choi, H. S.; Suh, S. B.; Cho, S. J.; Kim, K. S. *Proc. Natl. Acad. Sci. U.S.A.* **1998**, *95*, 12094–12099.

(8) Clegg, W.; Dale, S. H.; Hevia, E.; Hogg, L. M.; Honeyman, G. W.; Mulvey, R. E.; O'Hara, C. T. *Angew. Chem., Int. Ed.* **2006**, *45*, 6548–6550.

(9) (a) Dougherty, D. A. *Science (Washington, D.C.)* **1996**, *271*, 163–168. (b) Nakamura, R. L.; Anderson, J. A.; Gaber, R. F. *J. Biol. Chem.* **1997**, *272*, 1011–1018. (c) Dougherty, D. A.; Lester, H. A. *Angew. Chem., Int. Ed.* **1998**, *37*, 2329–2331. (d) De Wall, S. L.; Meadows, E. S.; Barbour, L. J.; Gokel, G. W. *Proc. Natl. Acad. Sci. U.S.A.* **2000**, *97*, 6271–6276.

(10) Macias, A. T.; Norton, J. E.; Evanseck, J. D. *J. Am. Chem. Soc.* **2003**, *125*, 2351–2360.

(11) Feller, D. *Chem. Phys. Lett.* **2000**, *322*, 543–548.

(12) Choi, H. S.; Kim, D.; Tarakeshwar, P.; Suh, S. B.; Kim, K. S. *J. Org. Chem.* **2002**, *67*, 1848–1851.

(13) Gokel, G. W.; De Wall, S. L.; Meadows, E. S. *Eur. J. Org. Chem.* **2000**, 2967–2978.

(14) Hu, J.; Barbour, L. J.; Gokel, G. W. *Chem. Commun.* **2001**, 1858–1859.

(15) Hu, J.; Barbour, L. J.; Gokel, G. W. *J. Am. Chem. Soc.* **2001**, *123*, 9486–9487.

(16) Allyl groups displaying both σ - and π -bonding have been observed in transition-metal complexes (e.g.: King, R. B.; Bisnette, M. B. *J. Organomet. Chem.* **1967**, *7*, 311–319. Müller, H. J.; Nagel, U.; Beck, W. *Organometallics* **1987**, *6*, 193–194. Beck, W.; Niemer, B.; Wieser, M. *Angew. Chem., Int. Ed. Engl.* **1993**, *32*, 923–949. Huffer, S.; Wieser, M.; Polborn, K.; Beck, W. *J. Organomet. Chem.* **1994**, *481*, 45–55. Gunnoe, T. B.; White, P. S.; Templeton, J. L. *Organometallics* **1997**, *16*, 3794–3799). The π -bonding in all these cases involves covalent d-electron bonding, not noncovalent cation– π interactions.

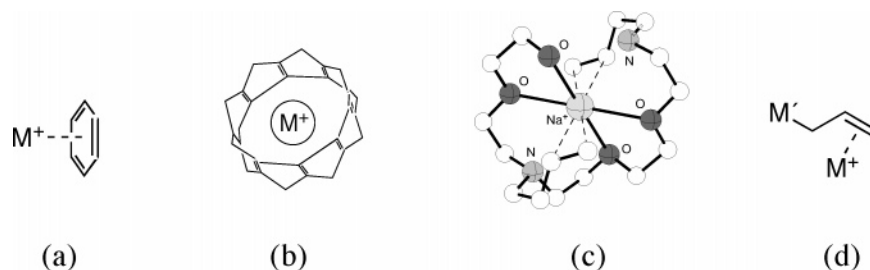


Figure 1. (a) Cation– π bonding to an aromatic ring. (b) Cation– π bonding in a beltene (cyclacene). (c) Na⁺ and allyl interaction in a lariat crown ether. (d) Simultaneous σ - and cation– π bonding with an allyl ligand.

Table 1. Crystal Data and Summary of X-ray Data Collection

	Li[Zn(1,3-(SiMe ₃) ₂ C ₃ H ₃) ₃]	Na[Zn(1,3-(SiMe ₃) ₂ C ₃ H ₃) ₃]	K[Zn(1,3-(SiMe ₃) ₂ C ₃ H ₃) ₃]
formula	C ₂₇ H ₆₃ LiSi ₆ Zn	C ₂₇ H ₆₃ NaSi ₆ Zn	C ₂₇ H ₆₃ KSi ₆ Zn
formula wt	628.62	644.67	660.78
cryst color	pale yellow	colorless	orange-red
cryst dims, mm	0.30 × 0.20 × 0.20	0.40 × 0.20 × 0.10	0.2 × 0.2 × 0.2
space group	<i>P</i> $\bar{1}$	<i>P</i> $\bar{1}$	<i>P</i> $\bar{1}$
cell dims			
<i>a</i> , Å	12.2863(6)	12.1734(17)	11.982(2)
<i>b</i> , Å	12.5849(7)	12.7745(18)	13.160(3)
<i>c</i> , Å	13.8068(7)	13.9023(19)	13.942(3)
α , deg	81.1310(10)	80.647(2)	79.258(3)
β , deg	71.0810(10)	71.666(2)	72.505(3)
γ , deg	88.5420(10)	88.586(2)	89.654(3)
<i>V</i> , Å ³	1994.67(18)	2024.1(5)	2057.1(7)
<i>Z</i>	2	2	2
calcd density, Mg/m ³	1.047	1.058	1.067
abs coeff, mm ⁻¹	0.809	0.809	0.877
<i>F</i> (000)	684	700	716
radiation type	Mo K α (0.710 73 Å)	Mo K α (0.710 73 Å)	Mo K α (0.710 73 Å)
temp, K	100(2)	173(2)	100(2)
limits of data collection, deg	1.58 < θ < 27.50	1.56 < θ < 28.26	1.56 < θ < 27.48
index ranges	−15 < <i>h</i> < 15, −16 < <i>k</i> < 16, −17 < <i>l</i> < 17	−15 < <i>h</i> < 16, −16 < <i>k</i> < 16, 18 < <i>l</i> < 18	−15 < <i>h</i> < 15, −16 < <i>k</i> < 16, −18 < <i>l</i> < 18
total no. of rflns collected	17 371	24 888	17 881
no. of unique rflns	8729 (<i>R</i> _{int} = 0.0190)	9119 (<i>R</i> _{int} = 0.0226)	8975 (<i>R</i> _{int} = 0.0203)
transmissn factors	0.7933–0.8549	0.7380–0.9235	0.8426–0.8426
no. of data/restraints/params	8729/0/316	9119/0/371	8975/0/316
<i>R</i> indices (<i>I</i> > 2 σ (<i>I</i>))	<i>R</i> = 0.0364, <i>R</i> _w = 0.0970	<i>R</i> = 0.0369, <i>R</i> _w = 0.0920	<i>R</i> = 0.0441, <i>R</i> _w = 0.1208
<i>R</i> indices (all data)	<i>R</i> = 0.0434, <i>R</i> _w = 0.1005	<i>R</i> = 0.0432, <i>R</i> _w = 0.0955	<i>R</i> = 0.0521, <i>R</i> _w = 0.1266
goodness of fit on <i>F</i> ²	1.060	1.082	1.071
max/min peak in final diff map, e/Å ³	+0.455/−0.338	+0.794/−0.479	+0.088/−0.496

back-bonding is also an important component of the metal–ligand interaction.

The allyl fragment is a potentially useful source of π -electrons in cation– π interactions, and Na⁺ has been found to bind to the allyl sidearms in the lariat crown ether *N,N'*-dibutenyl-1,10-diaza-18-crown-6 (Figure 1c).¹⁴ A similar role should be possible for allyl ligands in metal complexes, and we have found that metal-bound σ -allyl ligands can also engage in intramolecular cation– π interactions with an electropositive metal atom (Figure 1d).¹⁹ This combination of covalent and electrostatic bonding provides an environment in which the geometric requirements of multiple non-arene cation– π interactions can be studied.

(17) Krossing, I.; Reisinger, A. *Angew. Chem., Int. Ed.* **2003**, *42*, 5725–5728.

(18) Saarenketo, P.; Suontamo, R.; Jödicke, T.; Rissanen, K. *Organometallics* **2000**, *19*, 2346–2353.

(19) The largely noncovalent cation– π interaction should be distinguished from agostic interactions, whether the latter are conceived as the result of $3c-2e$ M \cdots H–C involvement (Brookhart, M.; Green, M. L. H. *J. Organomet. Chem.* **1983**, *250*, 395–408) or stem from the “negative hyperconjugative delocalization of the M–C bonding electrons” (Scherer, W.; McGrady, G. S. *Angew. Chem., Int. Ed.* **2004**, *43*, 1782–1806); neither of these definitions specifically require the presence of π -electron density on the ligands.

Experimental Section

General Considerations. All manipulations were performed with the rigorous exclusion of air and moisture using high-vacuum, Schlenk, or glovebox techniques. Proton (¹H) and carbon (¹³C) NMR experiments were obtained on a Bruker DPX-300 spectrometer at 300 and 75.5 MHz and a Bruker DPX-400 spectrometer at 400 and 100 MHz, respectively, and were referenced to residual proton and ¹³C resonances of THF-*d*₈ (δ 3.58 and 67.4), C₆D₆ (δ 7.15 and 128.1), and toluene-*d*₈ (δ 2.09 and 20.4). Lithium (⁷Li) NMR data were obtained at 155 MHz on the DPX-400 instrument and were referenced to external 1.0 M LiCl. Elemental analysis was performed by Desert Analytics (Tucson, AZ).

Materials. Hexanes were distilled under nitrogen from potassium benzophenone ketyl. Anhydrous tetrahydrofuran (THF) was purchased from Aldrich and used as received. Anhydrous metal salts were purchased from Strem Chemicals and used as received. C₆D₆, toluene-*d*₈, and THF-*d*₈ were vacuum-distilled from Na/K (22/78) alloy and stored over type 4A molecular sieves prior to use. Li[1,3-(SiMe₃)₂C₃H₃]₃ and K[1,3-(SiMe₃)₂C₃H₃]₃ were prepared by following published syntheses;²⁰ Na[1,3-(SiMe₃)₂C₃H₃]₃ was prepared from the transmetalation of the lithium salt with Na[*O-t*-Bu].

Synthesis of Li[Zn(1,3-(SiMe₃)₂C₃H₃)₃] (1). A 125 mL Schlenk flask equipped with a magnetic stir bar was charged with Zn(OTf)₂

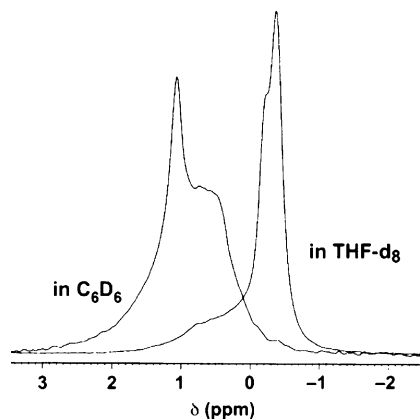


Figure 2. ^7Li NMR spectra of **1** in C_6D_6 and $\text{THF-}d_8$.

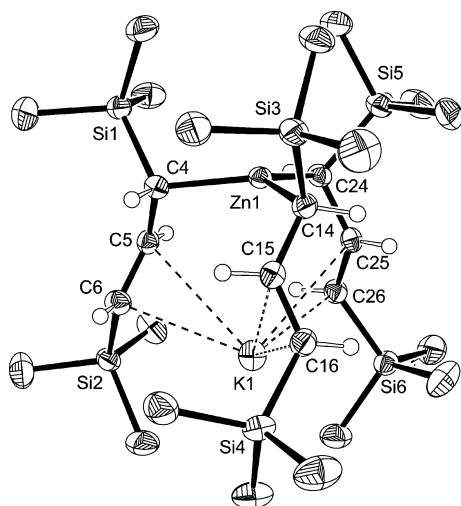


Figure 3. ORTEP drawing of **3**, with thermal ellipsoids at the 50% level. Hydrogen atoms have been removed from the trimethylsilyl groups for clarity. Selected bond distances (\AA) and angles (deg): Zn(1)–C(4), 2.065(2); Zn(1)–C(14), 2.065(2); Zn(1)–C(24), 2.075(3); C(4)–C(5), 1.467(3); C(5)–C(6), 1.358(4); C(14)–C(15), 1.460(3); C(15)–C(16), 1.355(3); C(24)–C(25), 1.460(3); C(5)–C(4)–Zn(1), 107.83(16); C(15)–C(14)–Zn(1), 108.71(16); C(25)–C(24)–Zn(1), 104.75(16).

(0.150 g; 0.413 mmol) in 30 mL of THF. $\text{Li}[1,3\text{-(SiMe}_3)_2\text{C}_3\text{H}_3]$ (0.238 g; 1.24 mmol) in 20 mL of THF was added to the dropping funnel. The apparatus was cooled to -78°C , after which the THF solution of $\text{Li}[1,3\text{-(SiMe}_3)_2\text{C}_3\text{H}_3]$ was added dropwise with stirring over the course of 15 min. The solution was warmed to room temperature overnight. Removal of solvent under vacuum, followed by extraction of the residue with hexanes, filtration of the extract over a medium-porosity glass frit, and removal of hexanes under vacuum afforded an air- and moisture-sensitive yellow solid (0.150 g, 58%). ^1H NMR (C_6D_6 , 298 K): δ 6.46 (t, $J = 14.1$ Hz, 3H, C_2), 3.50 (broad singlet, 6H, $\text{C}_{1,3}$), 0.15 (s, 54H, SiMe_3). ^{13}C NMR (C_6D_6 , 298 K): δ 137.67 (C_2 , central), 68.52 ($\text{C}_{1,3}$, outer), 1.36 (SiMe_3), 1.15 (SiMe_3).

Synthesis of $\text{Na}[\text{Zn}(1,3\text{-(SiMe}_3)_2\text{C}_3\text{H}_3)_3]$ (2**).** A 125 mL Schlenk flask equipped with a magnetic stir bar was charged with $\text{Zn}(\text{OTf})_2$ (0.152 g; 0.418 mmol) in 30 mL of THF. $\text{Na}[1,3\text{-(SiMe}_3)_2\text{C}_3\text{H}_3]$ (0.253 g; 1.21 mmol) in 20 mL of THF was added to the dropping funnel. The apparatus was cooled to -78°C , after which the THF solution of $\text{Na}[1,3\text{-(SiMe}_3)_2\text{C}_3\text{H}_3]$ was added dropwise with stirring over the course of 15 min. The solution was warmed to room

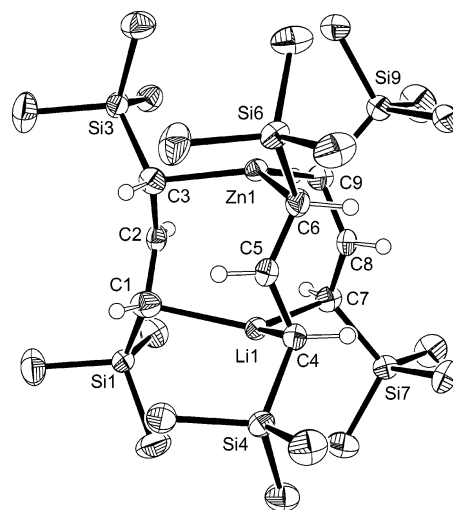


Figure 4. ORTEP drawing of **1**, with thermal ellipsoids at the 50% level. Hydrogen atoms have been removed from the trimethylsilyl groups for clarity. Selected bond distances (\AA) and angles (deg): Zn1–C3, 2.1101(19); Zn1–C9, 2.116(2); Zn1–C6, 2.1264(19); Li1–C4, 2.245(2); Li1–C7, 2.252(2); Li1–C1, 2.306(2); C2–C1–Li1, 95.24(13); C2–C3–Zn1, 98.99(12); C5–C4–Li1, 95.35(12); C5–C6–Zn1, 99.90(12); C8–C7–Li1, 92.69(12); C8–C9–Zn1, 101.50(12).

temperature overnight. Removal of the solvent under vacuum, followed by extraction of the residue with hexanes, filtration of the extract over a medium-porosity glass frit, and removal of hexanes under vacuum afforded an air- and moisture-sensitive yellow solid (0.220 g, 82%). Anal. Calcd for $\text{C}_{27}\text{H}_{63}\text{NaSi}_6\text{Zn}$: C, 50.30; H, 9.85; Na, 3.6. Found: C, 50.01; H, 9.85; Na, 3.0. ^1H NMR (C_6D_6 , 298 K): δ 7.59 (t, $J = 15.8$ Hz, 3H, C_2), 4.00 (broad singlet, 6H, $\text{C}_{1,3}$), 0.16 (s, 54H, SiMe_3). ^{13}C NMR (C_6D_6 , 298 K): δ 169.64 (C_2 , central), 77.8 (v br, $\text{C}_{1,3}$, outer), 0.99 (SiMe_3).

Synthesis of $\text{K}[\text{Zn}(1,3\text{-(SiMe}_3)_2\text{C}_3\text{H}_3)_3]$ (3**).** A 125 mL Schlenk flask equipped with a magnetic stir bar was charged with $\text{Zn}(\text{OTf})_2$ (0.567 g; 1.56 mmol) in 30 mL of THF. $\text{K}[1,3\text{-(SiMe}_3)_2\text{C}_3\text{H}_3]$ (1.05 g; 4.68 mmol) in 20 mL of THF was added to the dropping funnel. The apparatus was cooled to -78°C , after which the THF solution of $\text{K}[1,3\text{-(SiMe}_3)_2\text{C}_3\text{H}_3]$ was added dropwise with stirring over the course of 15 min. The solution was warmed to room temperature overnight. Removal of solvent under vacuum, followed by extraction of the residue with hexanes, filtration of the extract over a medium-porosity glass frit, and removal of hexanes under vacuum afforded an air- and moisture-sensitive, orange-red solid (0.880 g, 85%). Anal. Calcd for $\text{C}_{27}\text{H}_{63}\text{KSi}_6\text{Zn}$: C, 49.08; H, 9.61. Found: C, 48.66; H, 9.32. ^1H NMR (C_6D_6 , 298 K): δ 7.05 (t, $J = 15.3$ Hz, 3H, C_2), 3.42 (d, $J = 15.3$ Hz, 6H, $\text{C}_{1,3}$), 0.23 (s, 54H, SiMe_3). ^1H NMR ($\text{THF-}d_8$, 298 K, 300 MHz): δ 6.51 (t, $J = 15.0$ Hz, 3H), 3.19 (d $J = 15.0$ Hz, 6H), -0.054 (s, 54H, SiMe_3). ^1H NMR ($\text{tol-}d_8$, 298 K, 400 MHz): δ 6.95 (t, 3H, C_2), 3.33 (d $J = 15.2$ Hz, 6H), 0.15 (s, 54H, SiMe_3). ^{13}C NMR (C_6D_6 , 298 K): δ 163.91 (C_2 , central), 76.40 ($\text{C}_{1,3}$, outer), 1.00 (SiMe_3). Variable-temperature ^1H NMR ($\text{tol-}d_8$, 400 MHz, δ): 198 K, 7.1 (t, 3H), 0.28 (s, 54H, SiMe_3); 218 K, 7.06 (t, 3H), 3.38 (broad singlet, 6H), 0.25 (s, 54H, SiMe_3); 238 K, 7.04 (t, 3H), 3.36 (broad doublet, $J = 10.8$ Hz, 6H), 0.22 (s, 54H, SiMe_3).

Computational Details. All calculations were performed with the Gaussian 03W suite of programs.²¹ For the geometry optimization of **1**, the B3PW91 functional, which incorporates Becke's three-parameter exchange functional²² with the 1991 gradient-corrected correlation functional of Perdew and Wang,²³ was used. This hybrid functional has previously been shown to provide realistic geometries for organometallic species.^{24,25} The DFT-

(20) Simpson, C. K.; White, R. E.; Carlson, C. N.; Wroblewski, D. A.; Kuehl, C. J.; Croce, T. A.; Steele, I. M.; Scott, B. L.; Hanusa, T. P.; Sattelberger, A. P.; John, K. D. *Organometallics* **2005**, *24*, 3685–3691.

optimized double- ζ basis sets of Godbout²⁶ (DGDZVP2) were used with all atoms.

For analysis of the metal–benzene and metal–ethylene cations, an initial goal was the reproduction of the experimentally measured heats of formation of the gas-phase $[M(C_6H_6)]^+$ species ($M = Li, Na, K$). Trials with various functionals and basis sets lead to the selection of the hybrid PBE1PBE functional²⁷ and the use of basis sets of at least polarized double- ζ quality with diffuse functions on all C and H atoms. Somewhat better results (by 0.1–0.5 kcal mol⁻¹) were obtained if basis sets of triple- ζ quality (e.g., aug-cc-pVTZ) were used. The importance of including core valence correlation in reproducing binding energies in alkali-metal complexes²⁸ led to the use of the cc-pCVTZ basis sets on Li (11s,5p,2d,1f)/[4s,3p,2d,1f] and Na ((16s,10p,2d,1f)/[5s,4p,2d,1f]), and the corresponding “Feller Misc. CVTZ” on potassium ((18s,15p,4d,2f)/[8s,7p,4d,2f]) ((s,p) exponents from Ahlrichs;²⁹ polarization and core/valence exponents from Feller²⁸). Calculations on $[M(C_6H_6)]^+$ were performed under C_{6v} symmetry; trial calculations for $[M(C_2H_4)_n]^+$ were optimized to structures with nearly exact C_{2v} , D_{2d} , and D_3 symmetry for $n = 1-3$, respectively; the symmetry was made exact for subsequent work. All molecules were optimized with ultrafine grids and the GDIIS algorithm.³⁰ Small (less than 20i) imaginary frequencies were encountered in the $[M(C_2H_4)_2]_3^+$ calculations; these are considered to be artifactual. The other molecules displayed no imaginary frequencies; all geometries are considered to be minima on their potential energy surfaces.

General Procedures for X-ray Crystallography. Suitable crystals of $Li[Zn(1,3-(SiMe_3)_2C_3H_3)_3]$, $Na[Zn(1,3-(SiMe_3)_2C_3H_3)_3]$, and $K[Zn(1,3-(SiMe_3)_2C_3H_3)_3]$ were located, attached to glass fibers, and mounted on a Siemens SMART system for data collection. The intensity data were corrected for absorption (SADABS). All calculations were performed with the SHELXTL suite of programs.³¹ Final cell constants were calculated from a set of strong reflections measured during the actual data collection. Relevant crystal and data collection parameters for each of the compounds are given in Table 1. The space groups were determined from systematic absences and intensity statistics. The structures were solved by direct methods and refined against F^2 for all observed reflections, using SHELXS and SHELXL.³²

(21) Frisch, M. J.; Trucks, G. W.; Schlegel, H. B.; Scuseria, G. E.; Robb, M. A.; Cheeseman, J. R.; Montgomery, J. A., Jr.; Vreven, T.; Kudin, K. N.; Burant, J. C.; Millam, J. M.; Iyengar, S. S.; Tomasi, J.; Barone, V.; Mennucci, B.; Cossi, M.; Scalmani, G.; Rega, N.; Petersson, G. A.; Nakatsuji, H.; Hada, M.; Ehara, M.; Toyota, K.; Fukuda, R.; Hasegawa, J.; Ishida, M.; Nakajima, T.; Honda, Y.; Kitao, O.; Nakai, H.; Klene, M.; Li, X.; Knox, J. E.; Hratchian, H. P.; Cross, J. B.; Bakken, V.; Adamo, C.; Jaramillo, J.; Gomperts, R.; Stratmann, R. E.; Yazyev, O.; Austin, A. J.; Cammi, R.; Pomelli, C.; Ochterski, J. W.; Ayala, P. Y.; Morokuma, K.; Voth, G. A.; Salvador, P.; Dannenberg, J. J.; Zakrzewski, V. G.; Dapprich, S.; Daniels, A. D.; Strain, M. C.; Farkas, O.; Malick, D. K.; Rabuck, A. D.; Raghavachari, K.; Foresman, J. B.; Ortiz, J. V.; Cui, Q.; Baboul, A. G.; Clifford, S.; Cioslowski, J.; Stefanov, B. B.; Liu, G.; Liashenko, A.; Piskorz, P.; Komaromi, I.; Martin, R. L.; Fox, D. J.; Keith, T.; Al-Laham, M. A.; Peng, C. Y.; Nanayakkara, A.; Challacombe, M.; Gill, P. M. W.; Johnson, B.; Chen, W.; Wong, M. W.; Gonzalez, C.; Pople, J. A. *Gaussian 03*, revision C.02; Gaussian, Inc.: Wallingford, CT, 2004.

(22) Becke, A. D. *J. Chem. Phys.* **1993**, *98*, 5648–5652.

(23) Perdew, J. P.; Wang, Y. *Phys. Rev. B* **1992**, *45*, 13244–13249.

(24) Smith, J. D.; Hanusa, T. P. *Organometallics* **2001**, *20*, 3056–3062.

(25) White, R. E.; Hanusa, T. P. *Organometallics* **2006**, *25*, 5621–5630.

(26) Godbout, N.; Salahub, D. R.; Andzelm, J.; Wimmers, E. *Can. J. Chem.* **1992**, *50*, 560–571.

(27) Perdew, J. P.; Burke, K.; Ernzerhof, M. *Phys. Rev. Lett.* **1996**, *77*, 3865–3868.

(28) Feller, D.; Glendening, E. D.; Woon, D. E.; Feyereisen, M. W. *J. Chem. Phys.* **1995**, *103*, 3526–3542.

(29) Schaefer, A.; Horn, H.; Ahlrichs, R. *J. Chem. Phys.* **1992**, *97*, 2571–2577.

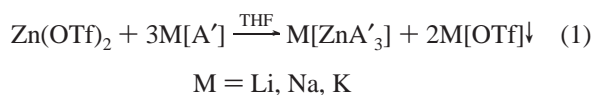
(30) Csanász, P.; Pulay, P. *J. Mol. Struct.* **1984**, *114*, 31–34. Farkas, O.; Schlegel, H. B. *J. Chem. Phys.* **1999**, *111*, 10806–10814.

(31) SHELXTL, version 6.1; Bruker Analytical X-Ray Systems, Madison, WI, 2000.

The similarity in chemical environments of the two metal-atom sites in $Li[Zn(1,3-(SiMe_3)_2C_3H_3)_3]$ and $Na[Zn(1,3-(SiMe_3)_2C_3H_3)_3]$ led to disorder in their occupancy. At each site there is 30% (for the Li complex) or 16% (for the Na complex) of the character of the other metal. The disorder was modeled using EADP and EXYZ commands that constrained the coordinates and thermal parameters to be identical for each pair, and the occupancies were constrained to unity.

Results and Discussion

Synthesis of Triallylzincates. Allyl ligands containing trimethylsilyl substituents are readily incorporated into thermally stable complexes with metals from across the periodic table,³³ and in an attempt to isolate trimethylsilylated allyl compounds of the group 12 metals, zinc triflate was treated with 2 equiv of the potassium salt of the bis(1,3-trimethylsilyl)allyl anion, $K[A']$ ($A' = [1,3-(SiMe_3)_2C_3H_3]$).²⁰ Potassium triflate was precipitated as a byproduct, and the triallylzincate $K[ZnA'_3]$ (**3**) was isolated instead of the intended neutral ZnA'_2 . Adjustment of the stoichiometry of the reaction (eq 1) and the use of lithium and sodium allyls as starting materials generated the air- and moisture-sensitive, yellow $Li[ZnA'_3]$ (**1**) and $Na[ZnA'_3]$ (**2**), in addition to the orange-red **3**, in moderate to good yields.



The formation of the zincate **3** when only 2 equiv of the allyl reagent was available is unusual, given that the parent $Zn(C_3H_5)_2$ is formed even with the use of 2.6 equiv of C_3H_5MgCl /equiv of $ZnCl_2$.³⁴ There are, however, several known cases in which reactions with electropositive metals and bulky allyl ligands do not give the stoichiometrically expected products.^{35,36} For example, in an attempt to synthesize $La[1,3-(SiMe_3)_2C_3H_3]_3$ from the reaction of 3 equiv of $K[1,3-(SiMe_3)_2C_3H_3]$ with $LaCl_3$, only $La[1,3-(SiMe_3)_2C_3H_3]_2Cl(thf)$ is produced.³⁵ Conversely, the triallyl complex $Y[1,3-(SiMe_3)_2C_3H_3]_3$ is formed when only 2 equiv of $K[1,3-(SiMe_3)_2C_3H_3]$ is treated with YCl_3 .²⁵ The strong σ -donation properties of the silylated allyl may encourage the formation of tri(allyl) species; the steric bulk of the substituents obviously does not interfere with the formation of the anion.

When a THF solution of **3** is treated with lithium iodide, precipitation of KI is accompanied by the formation of **1** (eq 2). Although the interaction of the Li^+ cation with the allyl anion



is likely stronger than with K^+ , this is probably only of minor importance to the metal exchange. The ion separation that occurs in THF (see below) and the precipitation of the insoluble KI are likely the dominant driving forces in the reaction.

(32) Sheldrick, G. M. SHELXS-97, SHELXL-97; University of Göttingen, Göttingen, Germany, 1997.

(33) Hanusa, T. P.; Carlson, C. N. In *Encyclopedia of Inorganic Chemistry II*; King, R. B., Ed.; Wiley: New York, 2005; Vol. 9, pp 5690–5695.

(34) Cheon, J.; Dubois, L. H.; Girolami, G. S. *Chem. Mater.* **1994**, *6*, 2279–2287.

(35) Woodman, T. J.; Schormann, M.; Bochmann, M. *Isr. J. Chem.* **2002**, *42*, 283–293.

(36) Quisenberry, K. T.; Smith, J. D.; Voehler, M.; Stec, D. F.; Hanusa, T. P.; Brennessel, W. W. *J. Am. Chem. Soc.* **2005**, *127*, 4376–4387.

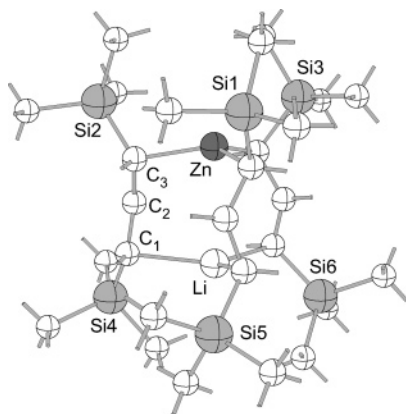


Figure 5. Calculated structure of **1** (B3PW91/DGDZVP2), with the numbering scheme used in the text. Bonds to hydrogen atoms are indicated as sticks. Selected bond distances (Å) and angles (deg): Zn–C₃, 2.081 Å; Li–C₁, 2.346 Å; C₂–C₁–Li, 90.79°; C₂–C₃–Zn, 102.08°; C₁–C₂–C₃, 129.90°.

Solution Behavior. The three zincates are fluxional in solution, as their ¹H and ¹³C NMR spectra at room temperature indicate that the structures are more symmetrical than in the solid state (see below), with apparently “ π -bound” allyl ligands. For example, the ¹H resonance for all six SiMe₃ groups in **3** appears as a singlet that broadens but does not split on cooling to –75 °C, and the hydrogen atoms on the carbons α and γ to the zinc appear as a doublet that coalesces to a single peak on cooling and disappears into the baseline by –75 °C. These fluxional rearrangements are reminiscent of the patterns observed in the neutral compound GaA₃³⁷ and indicate that the [ZnA₃][–] anion is free to undergo rearrangement largely uninhibited by the cation. The allyl ligands of **1** and **2** display the same highly symmetrical structure as does **3** in their ¹H NMR spectra, although the shifts are at different positions (e.g., in C₆H₆, the C–H triplet at δ 7.05 ppm for **3** appears at δ 7.59 ppm for **2**). Such shifts suggest that in C₆D₆ the cations remain associated with the triallylzinc anion.

Interestingly, in THF-*d*₈ the ¹H NMR chemical shifts for the three zincates are identical, indicating that the alkali-metal cations and the zincate anions are now largely solvent-separated. The change in solvation is apparent in the ⁷Li NMR spectra of **1** (Figure 2). In C₆H₆, a peak at δ 1.10 ppm is flanked by a broader resonance at δ 0.6 ppm, demonstrating that at least two similar environments exist for the Li⁺ cation, possibly the result of fluxional rearrangements or interaction with the benzene solvent. The shifts are typical for organolithium species (e.g., EtLi at δ 1.27; *i*-PrLi at δ 0.69).³⁸ In THF-*d*₈, the resonance shifts upfield to approximately δ –0.35 ppm and narrows. Although an upfield shift commonly occurs for alkyllithiums in polar solvents (that for EtLi is at δ 0.79 in Et₂O),³⁹ the shift in THF for **1** is substantial and is indicative of an increase in ionic character. The shift is not far from the value for the solvent-separated pair [Li(thf)₄][CPh₃] (–0.45 ppm in

THF-*d*₈; $\Delta\nu_{1/2}$ = 10.2 Hz),⁴⁰ although the width of the line in **1** ($\Delta\nu_{1/2}$ \approx 53 Hz) and the indications of some unresolved structure on the peak suggest that the latter species is not as symmetric.

Solid-State Structures. (a) Na[ZnA₃] (**2**) and K[ZnA₃] (**3**). Single-crystal X-ray structures of **2** and **3** (Figure 3) reveal that the three allyl ligands are bound to the zinc in an arrangement with approximate C₃ symmetry, with the alkali-metal cation situated between the three double bonds of the allyl ligands. The sodium derivative suffers from some disorder in the Na/Zn positions (see the Experimental Section for details), but it is unquestionably isostructural with the potassium salt; therefore, only **3** is discussed in detail here. The average Zn–C distance of 2.068(4) Å is similar to the Zn–C length of 2.09(2) Å found in the trialkyl anion Zn[CH(SiMe₃)₂]₃[–].⁴¹ The C–C and C=C bonds in the alkyl groups are localized at 1.462(5) and 1.359–(6) Å, respectively. The K⁺⋯C (olefin) contacts average 3.205–(3) and 2.945(3) Å to the carbon atoms β (C5, C15, C25) and γ (C6, C16, C26) to the zinc atom, respectively. These distances are comparable to the range of K⁺⋯C contacts usually observed with aromatic rings (cf. 3.02–3.35 Å to the benzyl group in {KZn[N(SiMe₃)₂]₂(CH₂Ph)}_∞⁴² or the 3.12–3.35 Å distances to the neutral arenes in {[K(toluene)₂]⁺[Mg(N(SiMe₃)₂]₃[–]]_n⁴³), although differences in coordination numbers make exact comparisons difficult.⁴⁴ The analogous Na⁺⋯C(olefin) contacts in **2** average 2.857(3) and 2.567(3) Å to the carbon atoms β and γ to the zinc atom, respectively, and are similar to known cation- π Na⁺⋯C(arene) distances (cf. 2.91 Å (av) in [Na₂(C₂-Ph₄)(OEt₂)₂]_n⁴⁵ or 2.88 Å (av) in (Et₂O)Na(Ph₂CCHCPh₂)⁴⁶). There are no contacts in either molecule that are suggestive of M⁺⋯C–H agostic interactions.

(b) Li[ZnA₃] (**1**). The single-crystal X-ray structure of **1** (Figure 4) is superficially similar to that of **1** and **2**. Like that of **2**, the structure of **1** is disordered over a twofold axis, but to a greater extent; refinement leads to occupancies of 70%(Zn)/30%(Li) for the atom marked “Zn1” and the reverse percentage for “Li1”. The general structural features of **1** are not in doubt, although some of the fine detail cannot be determined. For example, the average Zn–C distance of 2.117(3) Å is longer than in **3** and probably reflects the admixture of some Li–C character. Similarly, the direct lithium–carbon bond distance of 2.268(3) Å (av) is likely somewhat shorter than the undistorted value (but compare the 2.28 Å Li–C α bond found in {Li[CH₂CH₃]₄}.⁴⁷ The distances of lithium to the carbons β to the lithium (C2, C5, C8) range from 2.70 to 2.79 Å, which are distinctly longer than normal Li–C bonds. They are, however, similar to Li–aryl distances observed in (dibenzylamido)lithium, [(PhCH₂)₂NLi]_n (average 2.80 Å),⁴⁸ and in the chelating silazane [{Me₂Si(Ph)₂N–Li]₂, in which Li–C β distances range up to 2.77 Å.⁴⁹ Nevertheless, the marked

(40) Fernández, I.; Martínez-Viviente, E.; Breher, F.; Pregosin, P. S. *Chem. Eur. J.* **2005**, *11*, 1495–1506.

(41) Westerhausen, M.; Rademacher, B.; Schwarz, W. Z. *Anorg. Allg. Chem.* **1993**, *619*, 675–689.

(42) Clegg, W.; Forbes, G. C.; Kennedy, A. R.; Mulvey, R. E.; Liddle, S. T. *Chem. Commun.* **2003**, 406–407.

(43) Forbes, G. C.; Kennedy, A. R.; Mulvey, R. E.; Roberts, B. A.; Rowlings, R. B. *Organometallics* **2002**, *21*, 5115–5121.

(44) Mulvey, R. E. *Organometallics* **2006**, *25*, 1060–1075.

(45) Bock, H.; Ruppert, K.; Fenske, D. *Angew. Chem., Int. Ed. Engl.* **1989**, *28*, 1685–1687.

(46) Bock, H.; Ruppert, K.; Havlas, Z.; Fenske, D. *Angew. Chem., Int. Ed. Engl.* **1990**, *29*, 1042–1044.

(47) Dietrich, H. J. *Organomet. Chem.* **1981**, *205*, 291–299.

(48) Armstrong, D. R.; Mulvey, R. E.; Walker, G. T.; Barr, D.; Snaith, R.; Clegg, W.; Reed, D. *J. Chem. Soc., Dalton Trans.* **1988**, 617–628.

(49) Veith, M.; Koban, A.; Fries, K.; Spaniol, P.; Elsaesser, R.; Rammo, A.; Huch, V.; Kleinstaub, U. *Organometallics* **1998**, *17*, 2612–2618.

(37) Gren, C. K.; Hanusa, T. P.; Brennessel, W. W. *Polyhedron* **2006**, *25*, 286–292.

(38) Scherr, P. A.; Hogan, R. J.; Oliver, J. P. *J. Am. Chem. Soc.* **1974**, *96*, 6055–6059.

(39) Large downfield shifts are observed for cyclopentadienyllithium (>7 ppm) on moving from C₆D₆ to Et₂O, but this is a consequence of removal of the lithium from the aromatic ring current (Günther, H. In *Advanced Applications of NMR to Organometallic Chemistry*; Gielen, M., Willem, R., Wrackmeyer, B., Eds.; Wiley: Chichester, U.K., 1996; pp 247–290).

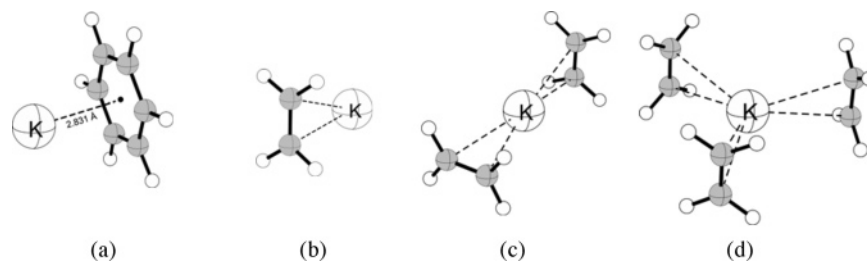


Figure 6. Optimized geometries of cation– π complexes: (a) $[\text{K}(\text{C}_6\text{H}_6)]^+$; (b) $[\text{K}(\text{C}_2\text{H}_4)]^+$; (c) $[\text{K}(\text{C}_2\text{H}_4)_2]^+$; (d) $[\text{K}(\text{C}_2\text{H}_4)_3]^+$.

Table 2. Calculated Energies^a for $[\text{M}(\text{C}_2\text{H}_4)]^+$

M ⁺	complex	energy (ΔH_{298})	protocol	ref
Li	$[\text{Li}(\text{C}_2\text{H}_4)]^+$	–18.99	MP2/6-31+G//MP2/6-31+G(d)	2
		–22.3	see text	this work
Na	$[\text{Na}(\text{C}_2\text{H}_4)]^+$	–12.36	MP2/6-31+G//MP2/6-31+G(d)	2
		–12.7	MP2/6-311+G(2d,2p)//MP2/6-31G(d)	56
		–14.6 ± 0.2	CCSD(T)/CBS (est)//MP2(FC)/CBS	11
		–14.9	see text	this work
		–10.7 ± 1.0	exptl (CID)	11
K	$[\text{K}(\text{C}_2\text{H}_4)]^+$	–7.05	MP2/6-31+G//MP2/6-31+G(d)	2
		–8.02	MP2/aug-cc-pVDZ//MP2/aug-cc-pVDZ	2
		–8.29	B3LYP/6-311+G(3df,2p)//B3LYP/6-31G(d)	52
		–8.9	see text	this work

^a In kcal mol^{–1}.

asymmetry of the Li–C distances in **1** suggests that the interaction of lithium is not strictly analogous to that of sodium or potassium but that more pronounced Li–C σ -bonding is involved.

Computational Studies. (a) Geometry of $[\text{Li}[\text{ZnA}'_3]]$. A model of **1** was examined at the B3PW91/DGDZVP2 level under C_3 symmetry in an attempt to reconstruct structural features of the undistorted molecule and to determine how much of the Li–C $_{\alpha}$ /C $_{\beta}$ bonding asymmetry might be ascribed to the solid-state disorder (Figure 5). The calculated Zn–C $_3$ distance of 2.081 Å is shorter than the solid-state value (2.117–(3) Å) and is now close to that in **3**. The Li–C $_1$ distance has lengthened somewhat to 2.346 Å, whereas the Li \cdots C $_2$ separation remains long at 2.737 Å. Using the optimized values and the experimentally determined occupancies of 70%/30% (see the Experimental Section), it is possible to calculate the “disordered” values as 0.70(2.081 Å) + 0.30(2.346 Å) = 2.16 Å for the Zn–C $_3$ distance (0.04 Å longer than the crystal structure) and 0.70(2.346 Å) + 0.30(2.081 Å) = 2.27 Å for the Li–C $_1$ distance (matches crystal structure). These values suggest that the geometry optimization has provided a credible restoration of the undistorted structure. The C–C and C=C double bonds of the allyl ligands, at 1.436(5) and 1.383(5) Å in the disordered crystal structure, have lengthened and shortened slightly in the optimized model to 1.455 Å (C $_2$ –C $_3$) and 1.378 Å (C $_1$ –C $_2$), respectively, supporting a largely localized model of the bonding.

(b) Geometry of Cation– π Interactions. DFT studies were conducted on model $[\text{M}(\text{C}_6\text{H}_6)]^+$ and $[\text{M}(\text{C}_2\text{H}_4)_n]^+$ complexes to assess geometric factors in the metal–allyl interactions of **1**–**3**. It has been noted that the gas-phase binding energies of Na⁺ to C $_2\text{H}_4$ (–10.7 kcal mol^{–1})¹¹ and C $_6\text{H}_6$ (–23.2 kcal mol^{–1})⁵⁰ are not in the ratio of 1:3 expected from the relative number of π electrons, a discrepancy partially ascribed to differences in geometry.² The three double bonds in the present triallylzincates are obviously able to interact with the alkali-metal cations in a way different from that of planar benzene, and an estimate of the relative binding energies would be instructive, as the number of available π electrons is the same in both cases.

There have been many previous computational investigations of $\text{M}^+\cdots\text{C}_6\text{H}_6$ interactions with a variety of ab initio and density functional methods.^{10,50–52} Although dispersion forces play a role in cation– π interactions, and current density functionals do not describe such forces well,⁵³ dispersion appears to have only a small influence in complexes of Li⁺ and Na⁺.^{2,54} In complexes involving K⁺, dispersion effects are more important but still represent only ~15% of the total interaction energies in $[\text{K}(\text{C}_6\text{H}_6)]^+$,² an amount that does not preclude DFT approaches from supplying usefully accurate energies in cation– π systems. We find that the hybrid PBE1PBE functional²⁷ combined with the basis sets of triple- ζ quality gives energies for the $[\text{M}(\text{C}_6\text{H}_6)]^+$ cations that are within the error limits of experimental values (see Table S1 in the Supporting Information).

To probe the effect of changing the number and orientation of π -bonds around the metals, the series of $[\text{M}(\text{C}_2\text{H}_4)_n]^+$ cations was investigated (Figure 6). The results of our DFT calculations are generally comparable to other calculations on alkaline-earth/ethylene complexes in the literature (Table 2), although they tend to be at the high end of binding strength. The only calculation of a $[\text{M}(\text{C}_2\text{H}_4)_3]^+$ species of which we are aware ($[\text{Na}(\text{C}_2\text{H}_4)_3]^+$)¹⁷ predicts a Na–C distance of 2.842 Å (BP86/TZVPP level), 0.053 Å longer than our value of 2.789 Å. We are unaware of any previous calculations for $[\text{M}(\text{C}_2\text{H}_4)_2]^+$ complexes.

(50) Amicangelo, J. C.; Armentrout, P. B. *Int. J. Mass Spectrom.* **2001**, *212*, 301–325.

(51) (a) Feller, D.; Dixon, D. A.; Nicholas, J. B. *J. Phys. Chem. A* **2000**, *104*, 11414–11419. (b) Quinonero, D.; Garau, C.; Frontera, A.; Ballester, P.; Costa, A.; Deya, P. M. *J. Phys. Chem. A* **2005**, *109*, 4632–4637. (c) Nicholas, J. B.; Hay, B. P.; Dixon, D. A. *J. Phys. Chem. A* **1999**, *103*, 1394–1400.

(52) Lau, J. K.-C.; Wong, C. H. S.; Ng, P. S.; Siu, F. M.; Ma, N. L.; Tsang, C. W. *Chem. Eur. J.* **2003**, *9*, 3383–3396.

(53) (a) Kristyán, S.; Pulay, P. *Chem. Phys. Lett.* **1994**, *229*, 175–180. (b) Koch, W.; Holthausen, M. C. *A Chemist's Guide to Density Functional Theory*, 2nd ed.; Wiley: New York, 2001. (c) Johnson, E. R.; Wolcok, R. A.; DiLabio, G. A. *Chem. Phys. Lett.* **2004**, *394*, 334–338.

(54) Zierkiewicz, W.; Michalska, D.; Cerny, J.; Hobza, P. *Mol. Phys.* **2006**, *104*, 2317–2325.

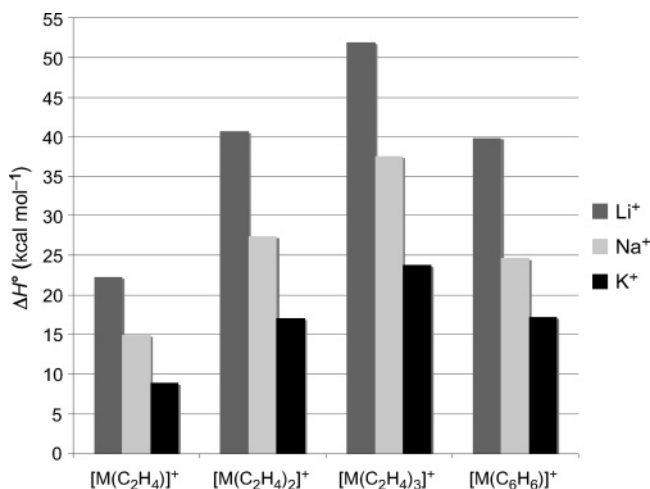


Figure 7. Calculated enthalpies of formation (ΔH°) of $[M(C_2H_4)_n]^+$ and $[M(C_6H_6)]^+$ (PBE1PBE/TZV).

An examination of the trends in binding enthalpies (Figure 7) is instructive. As expected for a largely ionic interaction, the enthalpies decrease in the order $Li^+ > Na^+ > K^+$. There is a roughly additive increase in the interaction energy with each additional ethylene molecule, averaging 20, 14, and 8 kcal mol⁻¹ for Li, Na, and K, respectively. It is also clear that three ethylene molecules arranged around the metal center interact more strongly than does a single benzene molecule, presumably because only one face of the metal cation is involved with the latter. In fact, two ethylene molecules arranged on either side of the metal interact approximately as strongly as does a benzene molecule. Of course, this result must be tempered by the fact that the free energies of formation of $[M(C_6H_6)]^+/[M(C_2H_4)_3]^+$ are always greater for the benzene complexes than for those with ethylene (e.g., -17.6 kcal mol⁻¹ ($[Na(C_6H_6)]^+$) and -12.8 kcal mol⁻¹ ($[Na(C_2H_4)_3]^+$); see the Supporting Information for other cases), owing to the larger number of ethylenes involved. Such comparisons are also complicated by the fact that in the zincates the olefinic functionalities are not completely independent ligands, thus limiting that entropic contribution to the energy.

Conclusions

The determination that the olefinic functionality of a σ -bound allyl ligand can engage in cation- π interactions with a second, dissimilar metal establishes a new combination of bonding modes for the allyl anion in metal complexes and new coordination environments for the alkali-metal cations. It is possible that similar bonding exists in related complexes with unsubstituted allyl ligands, e.g., $BrMg[Zn(C_3H_5)_3]$,⁵⁵ but this has not been crystallographically established.

In the attempt to understand the formation of the alkali-metal triallylzincates, it should be stressed that a principal driving force is the electrostatic attraction between the cations and the $[ZnA'_3]^-$ anion. Although the model $[M(C_2H_4)_n]^+$ complexes are not perfect analogues of the zincates, the finding from density functional studies that two olefinic bonds arranged in a staggered manner around an alkali metal are roughly equal in binding enthalpy to a benzene ring, and that three olefinic units around a metal can surpass the arene binding enthalpy by 30% or more, highlights the importance of geometrical factors in cation- π interactions. It suggests that their strength could be improved through judicious ligand design. The changes in the types of cation- π interactions formed between A'_3Zn^- and related A'_3M^- species with other monovalent and divalent metals are being examined.

Acknowledgment. We thank the donors of the Petroleum Research Fund, administered by the American Chemical Society, and the National Science Foundation for support of this research.

Supporting Information Available: CIF files giving X-ray crystallographic data for **1–3**. This material is available free of charge via the Internet at <http://pubs.acs.org>.

OM061174D

(55) Sugimura, H.; Watanabe, T. *Synlett* **1994**, 175–177.

(56) Hoyau, S.; Norrman, K.; McMahon, T. B.; Ohanessian, G. *J. Am. Chem. Soc.* **1999**, *121*, 8864–8875.